Continuous Flow Analysis of Total Organic Carbon in Polar Ice Cores

URS FEDERER,*,†,‡
PATRIK R. KAUFMANN,†,‡
MANUEL A. HUTTERLI,§
SIMON SCHÜPBACH,†,‡ AND
THOMAS F. STOCKER*,†,‡

Climate and Environmental Physics, Physics Institute, University of Bern, Bern, Switzerland, Oeschger Centre for Climate Change Research, University of Bern, Bern, Switzerland, and British Antarctic Survey, Cambridge, United Kingdom

Received May 6, 2008. Revised manuscript received September 2, 2008. Accepted September 3, 2008.

Ice cores are a widely used archive to reconstruct past changes of the climate system. This is done by measuring the concentration of substances in the ice and in the air of bubbles enclosed in ice. Some species pertaining to the carbon cycle (e.g., CO_2, CH_4) are routinely measured. However, information about the organic fraction of the impurities in polar ice is still very limited. Therefore, we developed a new method to determine the content of total organic carbon (TOC) in ice cores using a continuous flow analysis (CFA) system. The method is based on photochemical oxidation of TOC and the electrolytic quantification of the CO_2 produced during oxidation. The TOC instrument features a limit of detection of 2 ppbC and a response time of 60 s at a sample flow rate of 0.7 mL/min and a linear measurement range of 2−4000 ppbC. First measurements on the ice core from Talos Dome, Antarctica, reveal TOC concentrations varying between 80 and 360 ppbC in the 20 m section presented.

Introduction

For many years, the analysis of ice cores has been recognized as an important source of information for the understanding of the global climate system and in quantifying the range of past natural and anthropogenic changes in atmospheric chemistry and composition (*1*). Much information about conditions and processes of the past climate are archived at high temporal resolution in ice cores and cover a relatively long time span of up to 800 kyr back into the past (*2, 3*).

Organic compounds play an important role in cloud formation and atmospheric acidification (*4, 5*). Furthermore, they can make up the majority of the total suspended particle mass in some parts of the world and can significantly contribute to the global radiation budget (*6*). In contrast to the content of major ions of polar snow and ice (*7*), organic material is one of the least understood fractions of the aerosol load deposited on a polar ice sheet. This despite the fact that the content of organic impurities of ice cores can outweigh the sum of ions (*7*).

Due to the extreme diversity of different organic compounds present in the atmosphere (*8*) and thus in polar ice cores (*9, 10*), it is very challenging to characterize the composition of the organic carbon content. Only a minor fraction has been specified so far and existing studies mainly focus on individual compounds such as formaldehyde (*11, 12*), methansulfonate (*13*), low molecular weight organic acids (*14*), or fatty acids (*15, 16*). The goal of this work is to address this lack of measurements of organic carbon in polar ice, and to develop a new device to determine total organic carbon (TOC) by continuous flow analysis (CFA).

One of the major advantages of the CFA technique (*17, 18*) is the ability to provide a meltwater stream which was melted continuously under controlled conditions and was never exposed to the atmosphere (*19*). For this, an ice sample with a typical square cross section of 32 × 32 mm^2 and a length of 1 m is placed on top of a melt head to create a continuous melt flow which consists of a water flow segmented by the air present in the ice. The upper surface of the melter head is divided into two concentric parts, and to prevent any contamination, only the debubbled sample water from the inner part is used for the CFA methods as well as the TOC analysis described here.

Because of the presence of organic compounds in the drilling fluid, laboratory air, and packing materials, decontamination of discrete samples for organic analysis is challenging and very time-consuming. CFA is thus in general much more efficient compared to discrete sampling methods, typically allowing a depth resolution of ∼1 cm over the full length of a deep ice core (∼3 km). However, CFA methods require a very high sensitivity adequate for the low impurity concentrations present in polar ice cores, a fast response time (seconds to at most a couple of minutes) and very low water consumption (maximum of ∼1 mL/min typically available per channel).

The analysis of TOC includes the conversion of organic compounds to CO_2 and its subsequent quantification. For the conversion either high-temperature combustion, chemical- or UV-oxidation can be used (*20, 21*), whereas the CO_2 is measured using conductometry or IR absorption spectrometry. For all these methods commercial analyzers are available but they do not meet all of our requirements such as continuous flow operation, sample and reagent consumption, precision, response time, portability, and customer serviceability, which is critical during field deployments.

In this work, we present a new CFA method designed for measuring the concentration of total organic carbon (TOC) in polar ice cores. The method is based on a continuous photochemical oxidation of organic molecules in the sample water flow with subsequent quantification of the CO_2 produced. This is performed by measuring the electrolytic conductivity. The method was successfully embedded into our established CFA system (*17, 18*) and applied during a measurement campaign. Below we describe the new method and its analytical characteristics and present the first measurements made on the ice core from Talos Dome, Antarctica.

Materials and Methods

Analytical Setup. The detection of TOC in the air-free sample water stream provided by the melting system (*17*) consists of three steps: The UV oxidation, the transfer of the CO_2 produced into a carrier flow, and its subsequent detection by measuring the electrolytic conductivity.

After mixing the sample flow with the reagent (0.4 M phosphoric acid), it is split in two channels determining the content of total carbon (TC) and total inorganic carbon (TIC), respectively (Figure 1). TIC includes the inorganic CO_2

* Corresponding author e-mail: federer@climate.unibe.ch.
† Physics Institute, University of Bern.
‡ Oeschger Centre for Climate Change Research, University of Bern.
§ British Antarctic Survey.

10.1021/es801244e CCC: $40.75
Published on Web 10/04/2008

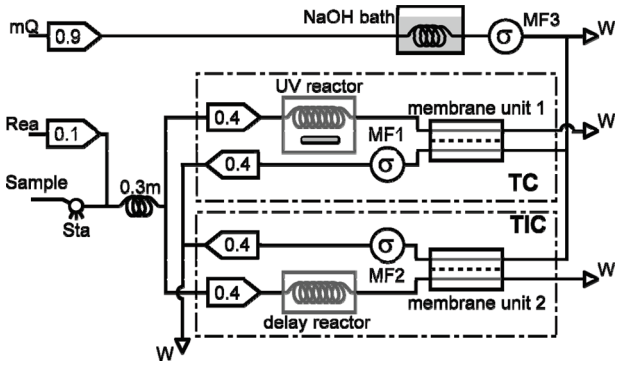

FIGURE 1. Schematic setup of the TOC detection system. After continuous mixing with reagent, the sample water is divided into two lines: "TC" equipped with an UV lamp and "TIC" constructed in the same way as "TC" but without lamp. The TOC value is calculated as the difference between total carbon (TC) and total inorganic carbon (TIC). Abbreviations and symbols: reagent (Rea), solenoid valve (small white circle), working standards (Sta), pump tubings and flow directions (arrow boxes), flow rates in mL/min (numbers in the arrow boxes), measuring cells (MF) for the electrolytic conductivity (σ in white circles), waste (W).

originating from the ice and the air bubbles, TC further includes the additional CO_2 produced by the oxidation of the organic molecules in the sample water.

Both channels are virtually identical, except for the photo-oxidation of the organic material in the TC line, using a strong UV source (Figure 1, see the Oxidation Reactor section). If all organic carbon (dissolved organic carbon, DOC, and particulate organic carbon, POC) is oxidized, TOC can be calculated as the difference of the two signals as

$$\mathrm{TOC} = \mathrm{TC} - \mathrm{TIC} \quad (1)$$

this is, strictly speaking, the UV-oxidizable OC of our sample. The whole analytical manifold is made of 1/16" × 0.5 mm PFA and PEEK tubing (from Omnilab and Upchurch). Tygon pump tubing is used in a peristaltic pump (both from Ismatec SA) for all flow lines.

The continuous sample flow of 0.7 mL/min is acidified with the reagent at a flow rate of 0.1 mL/min to reduce the pH of the sample stream to pH < 2. The reagent and the standard solution are from Merck and prepared with ultra pure Milli-Q water from a Millipore Gradient A10 (resistance of ≥18.2 MΩ/cm) with integrated UV lamp to reduce the organic content of the water to the lower ppbC range.

Special attention was directed to minimizing mixing volumes as well as tubing length in order to keep the dispersion, which limits the temporal resolution and thus the depth resolution in the ice, as small as possible.

Oxidation Reactor. The TOC content of the sample flow is converted to CO_2 by UV oxidation. The oxidation reactor consists of a custom-made octagonal glass coil (17 windings) made of quarz capillary (Ilmasil PS, length of 150 cm; i.d., 0.6 mm; o.d., 1.0 mm, from Quarzschmelze Ilmenau). In one of the two channels, the coil is exposed to UV light from a low-pressure mercury UV lamp (wavelength of 254 and 185 nm, NNQ8/18, from Hereaus). The optical transmissivity of the coil is above 0.95 at both wavelengths, due to a very small wall thickness. The sample residence time in the reactor is about 1 min at the chosen flow rate of 0.41 mL/min of the sample-reagent mixture.

A custom-made connection between the thin-walled quarz capillary tube and the PEEK tubing, using an adhesive agent with very low outgassing properties (TorrSeal, from Varian), was deployed because equivalent connectors are not commercially available.

Ozone has strong optical absorbing properties for UV light and would reduce the efficiency of the reactor. Therefore, and to eliminate the potential health hazard of ozone, the reactor body is flushed with an unreactive gas like N_2 or He preventing ozone production from ambient air. It is critical to avoid an unequal cooling of the UV lamp as this would result in a blow out of the lamp. The radiation intensity is monitored by a GaP-UV-photodiode (EPD-150−0, from Roithner) to ensure constant oxidation conditions.

The photochemical processes during the UV oxidation affect the organic molecules in two ways. While the 185 nm-irradiation produces highly reactive radicals like OH and HO_2 by the radiolysis of water and oxygen, the 254 nm-irradiation attacks mainly UV-sensitive areas of organic molecules (*22*). In contrast to existing instruments, the oxidation efficiency in the reactor was not further enhanced with persulfate reagents (*23*) or additional heating. Although the oxidation time of ∼1 min is relatively short compared to other UV photo-oxidation methods (*24*) the determined oxidation efficiencies for the various chemical compounds tested (see the Characteristics section) indicate a rather complete oxidation. This result was checked by a filtering experiment and a comparison with a commercially available analyzer (see Characteristics section).

Extraction of CO_2. After the oxidation reactor, the CO_2 is extracted in the TC and also in the TIC channel by a selective membrane unit and redissolved in a high purity water flow (carrier flow, see Figure 1). This is necessary to remove the background conductivity stemming from the ions present in the ice core and the reagent and to remove potential interferences of byproducts other than CO_2 formed during the oxidation. To enhance the extraction efficiency and maintain constant pH conditions, the meltwater is acidified to pH < 2 so that the dissolved carbonates are present as CO_2. The membrane unit consists of a silicone rubber tube (110 mm; i.d., 0.5 mm; o.d., 0.7 mm, from Labomatic) which divides the inner volume of a Pyrex glass tube (150 mm; i.d., 1.0 mm) into two parts. The sample water flow inside the rubber tube is pumped in opposite direction to the carrier flow in the volume between the rubber and glass tube. Because silicon rubber has a high permeability for CO_2 compared to other gases (*25, 26*), CO_2 is selectively extracted from the sample flow and transferred into the carrier flow.

To reduce wall thickness and thus to enhance the CO_2 permeation through the membrane, the silicone rubber tube is stretched by about a third in length. Before installation, the silicone rubber tube has to be rinsed thoroughly with Milli-Q water to ensure a good wetting of the membrane surface, to avoid micro bubbles sticking on the surface and hence disturbing the flow and the membrane diffusive characteristics.

Prior to the extraction membrane, the carrier flow (Milli-Q water) is decarbonated in a carbonate removal unit. Therein, a silicon rubber tube (3 m; i.d., 0.5 mm; o.d., 0.7 mm) is immersed in NaOH solution (0.2M) which acts as a trap for CO_2. To monitor the purification, the electrolytic conductivity is subsequently measured (see Figure 1 and the Detection section for details) which indicates a TIC content of a sub-ppbC level.

Detection. After the extraction of CO_2 from the sample flow and redissolution into the carrier flow, the carbonate equilibria

$$CO_2 + H_2O \leftrightarrow H^+ + HCO_3^- \leftrightarrow 2H^+ + CO_3^{2-} \quad (2)$$

are established. Subsequently, the electrolytic conductivity σ of the carrier flow is measured and thus the carbon content can be calculated (*27*). For this, two conductivity meters (AS1056) are used in combination with two Micro Flow Cells (Nr.529, with a cell constant of 100 cm^{-1} and a volume of 120 μL, both from Amber Science), one for each of the TIC and TC line (Figure 1). The value of TOC is then determined as the difference of TC and TIC (see the Convolution of the

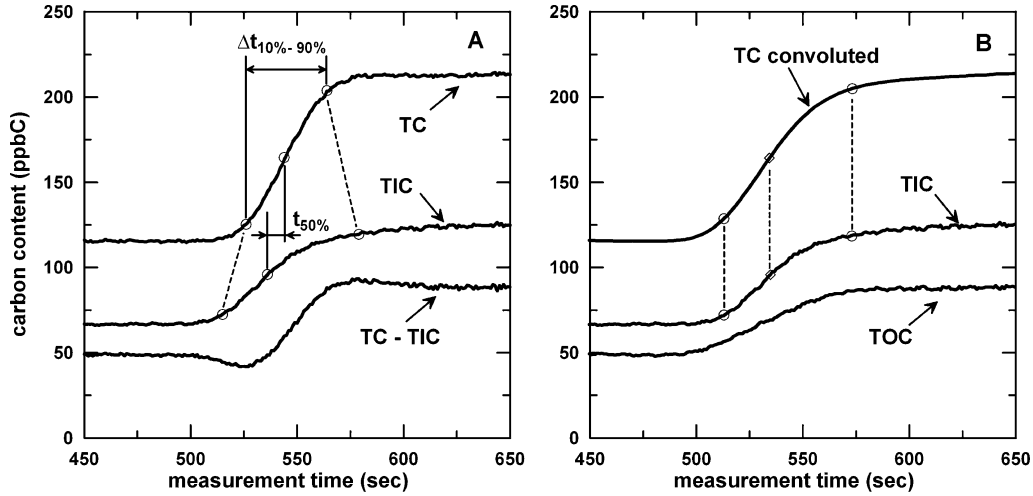

FIGURE 2. Example of the measurement of a 39 ppbC TOC standard. (A) Data of TC and TIC without correction, together with the difference TC-TIC. Under- and overshooting of the difference signal are clear artifacts caused by an insufficient synchronicity of the TC and TIC signals (B) Convolved TC signal and the resulting TOC data.

Signals section).

In order to avoid a signal drift due to temperature changes, the cells are stabilized at 30 ± 0.05 °C. They are mounted on a copper piling which is heated with heating foil (from Minco), controlled by a thermostat (dTron16, from Jumo). The conductivity cells are calibrated with 3 different dilutions of a 718 μS/cm−KCl standard solution (from Amber Science).

Convolution of the Signals. Because the TOC signal is calculated as the difference of TC and TIC, it is crucial to ensure that both signals show an identical dynamic response behavior (Figure 2B) to avoid artificial peaks due to asynchrony of the TC and TIC signals (Figure 2A). The synchronicity of the two signals should be maintained regarding signal timing as well as response time, i.e., the rise times from one level to another. Therefore, special attention was drawn to the identical mechanical manufacturing and tubing of the system. The semipermeable membrane is a major source of uncertainty, because the characteristics of the permeation of the CO_2 strongly depend on the wall thickness of the membrane (0.1 mm), which is not available with the necessary tolerances.

To correct for effects caused by this, the signal with the shorter risetime $\Delta t_{(10\%-90\%)}$ is convolved with a transfer function (e.g., TC in Figure 2), so that the rise times are identical and the midpoints $t_{(50\%)}$ are coincident. For the transfer function f we assume

$$f(t) = a \times \exp(-(t)/b),\ t>0 \qquad (3)$$

the parameters a and b were optimized so that $\Delta t_{(10\%-90\%)}$ and $t_{(50\%)}$ of both signals differ at most by 1 s. An example is shown in Figure 2B, where the TC signal has been convolved and the under- and overshooting of the TOC signal has vanished. For every standard run performed with a TOC standard, the parameters a and b in eq 3 are redetermined which is especially important after maintenance of the system or repair. We estimate the influence of different parameters to our TOC data, determined by different calibrations, to about ± 2% (see Supporting Informations for details).

Results and Discussion

Characteristics. The new TOC analysis unit features excellent linearity ($r^2 > 0.998$) over the whole measurement range from the limit of detection (LOD) of 2 ppbC to 4000 ppbC (see Supporting Information). LOD is calculated as three times the standard deviation of the signal of Milli-Q water (∼50 ppbC). Above 4000 ppbC, the rise of the signal diminishes rapidly with increasing concentrations likely due to saturation effects of the semipermeable membrane. The standard series was measured with different dilutions of a TOC standard (1000 mg/L, from Merck), containing potassium hydrogen phthalate ($C_8H_5KO_4$), which is likely stabilized with sodium azide (NaN_3) to minimize biological activity (information is not released from Merck).

The precision was determined by measuring alternately two standards of 48.8 and 126.1 ppbC for 10 times and calculating the standard deviation which yielded values of 1.1 and 3.0 ppbC, respectively. The interference of other compounds was checked with various species of ions and molecules such as Na^+, NH_4^+, Ca^+, K^+, H_2O_2, NO_3^-, Cl^- at concentrations which are commonly found in ice cores. Very low interferences of those species in the range of the resolution of the TOC measurement were found, indicating that matrix effects in the meltwater are negligible.

In order to investigate the efficiency of the oxidation processes of different organic molecules, various chemical compounds with different functional groups, bond structures and chain lengths were analyzed (Figure 3). The resulting efficiencies are relative to the efficiency of the TOC standard (set to 100%) and range from 86 to 139%. Especially for abundant species in ice cores like formic acid and acetic acid (*7*), the oxidation efficiencies are very close to the TOC standard.

The temporal resolution of the method defined as the time the signal needs to rise from 10 to 90% of a concentration step from Milli-Q water to a standard solution level is about 60 s. This corresponds to a depth resolution of ∼3.5 cm at a typical melting speed of 3.5 cm/min. This is a considerably higher value than for other analytical CFA units (*17*) due to a long flow path and the membrane unit, which involves diffusive processes. However, at the same time, the depth resolution is much higher than what can be achieved in the same time by a discrete method, and can, e.g., still provide subannual resolution at high accumulation sites.

For a further characterization of our data, a filtering experiment with a natural water sample (melted ice from the Dye-3 ice core, Greenland) was conducted. We used a hydrophilic PTFE filter (0.45 μm, Millex-LCR from Millipore) to remove POC from the sample. The unfiltered sample revealed a TOC value of 204.1 ppbC and 7% less (189.9 ppbC) for the filtered sample. This POC content is consistent with previous measurements (*28*) showing that our instrument measures TOC and not only the DOC. However, these results suggest that POC in Polar ice cores only contributes a minor fraction to the TOC.

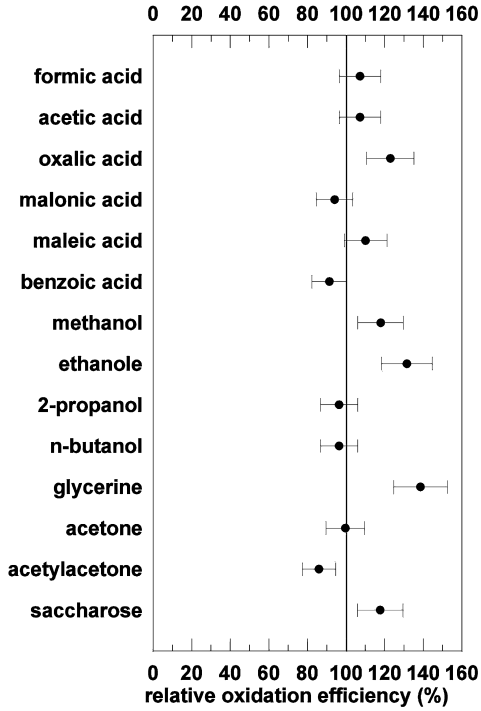

FIGURE 3. The oxidation efficiencies of different organic molecules relative to the potassium hydrogen phthalate (PHP) TOC standard (set to 100%). For each molecule three different dilutions in the concentration range of 20−130 ppbwC were measured. Shown error bars of ±10% are larger than the resolution of the system, because they include the uncertainties introduced by the dilutions of the pure chemical substances.

In order to compare our TOC instrument with existing analyzers, we performed measurements with a natural water sample (melted ice from the Dye-3 ice core, Greenland) with a Sievers 900 TOC analyzer. The results are 144.6 ppbC for our system and 154.7 ppbC for the Sievers 900 (results are mean values of three measurements). There is no significant difference between the measured values, also considering the necessary transfer of the sample to specific vials for the Sievers 900 (certified to 10 ppbC).

These results indicate that our new system quantitatively measures TOC.

First Measurements. The first meters of the Talos Dome ice core drilled in 2006 (*29*), were measured with the new TOC instrument. Measurements of a section of 20 m from a depth of 328−348 m (of an age of ∼4500 yr. BP) are shown in the upper panel of Figure 4. TOC values range from 80 to 360 ppbC with a small but significant decreasing trend with depth. The CFA system, including TOC, was calibrated every 4 m of ice (i.e., ∼ every 2 h).Therefore we can exlude that the trend is a measurement artifact. On the same ice core, the components of Ca^{2+}, Na^+ and NH_4^+ were measured with CFA and for comparsion with TOC data the section from 329 to 330 m is shown in the lower panel of Figure 4. NH_4^+ in Antarctic ice cores is thought to represent the marine biological activity in the Southern ocean (*30*), whereas Na^+ is interpreted as a proxy for sea ice extent and production (*31*). Ca^{2+} has been corrected according to the empirical calibration by (*32*) for the sea salt contribution to the total calcium content. The remaining $nssCa^{2+}$ represents the mineral dust fraction to total Ca^{2+}. Neither the trend nor the high-frequency variations of TOC are correlated with any of the other records measured. For example, a significant TOC peak at 329.1 m is not imprinted in the other records and vice versa clear peaks in Na^+ and $nssCa^{2+}$ have no counterparts in the TOC record indicating different sources, seasonality of the sources, and/or transport and deposition

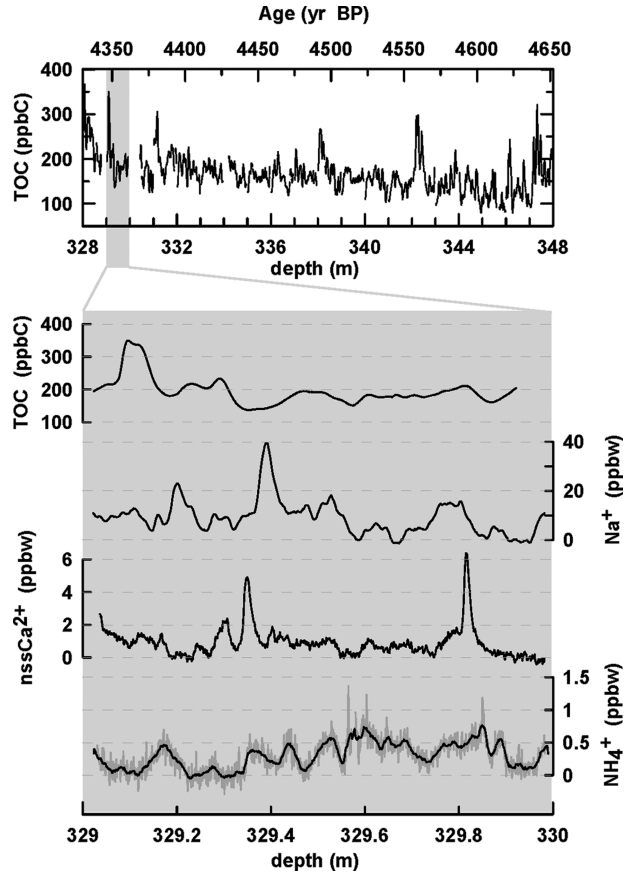

FIGURE 4. Upper panel: a section of 20 m of TOC data from the Talos Dome ice core. The data are plotted on a preliminary age scale (personal communication, F. Parrenin). Gaps in the data result from breaks in the ice core or contamination. Lower panel: a detailed plot of TOC together with the established CFA components $nssCa^{2+}$, Na^+ and NH_4^+ from 329 to 330 m. To reduce the electronic noise of NH_4^+ (gray), the data has been smoothed with a 13 mm running mean (black line). All other data are shown in 1 mm spacing.

patterns. In the future we plan to measure specific organic compounds such as HCHO and organic acids or oxidizing compounds such as H_2O_2 with our CFA system in parallel to TOC to study their contribution to the TOC record.

Clearly illustrated in the enlargement in Figure 4 is the lower spatial resolution of the TOC measurement compared to the other species. While Na^+ and $nssCa^{2+}$ would in principle allow resolving annual cycles at Talos Dome (with an annual snow accumulation of about 7.5 cm ice equivalent), this is not possible with the TOC sensor. Note, however, that the resolution of annual cycles in ice cores is not only dependent on the nominal resolution of the method but is also limited by the amplitude of seasonal cycles at a specific site and on the degree of snow reworking, as reflected in the weak seasonal variability of those species in Figure 4. Longer-term variations on multiannual to orbital time scales, however, can be reliably resolved in TOC and other species. With a further tuning of the response time, the developed system has the potential to resolve annual cycles.

The new TOC analyzer has a measurement range 2−4000 ppbC and a temporal resolution of about 1 min, thus fulfilling the requirements for CFA on Polar ice cores with respect to time resolution and sensitivity. Interferences from major ions are low enough not to be relevant for Polar ice core analyses. The instrument was embedded into an existing CFA setup and first measurements have been carried out successfully on the Talos Dome ice core. Comparison measurements with a commercially available TOC analyzer imply accurate TOC

values of our new system. Measured TOC values varied between 80 and 360 ppbC over the 20 m of data shown. Obtained values are in good agreement with results from other studies which report discrete values in the same order of magnitude for polar snow and ice (*10, 33, 34*). Quantification of the organic content of polar ice cores will be very helpful in further characterizing past changes in the carbon cycle.

Acknowledgments

Financial support by the Swiss National Science Foundation is acknowledged. Talos Dome Ice core Project (TALDICE), a joint European programme, is funded by national contributions from Italy, France, Germany, Switzerland and the United Kingdom. Main logistical support was provided by PNRA. We thank Remo Walther, Hans-Peter Moret, and Peter Nyfeler for technical support and the anonymous reviewers and Hubertus Fischer for their fruitful comments. This document was produced with the financial help of the Prince Albert II of Monaco Foundation.

Note Added after ASAP Publication

The Acknowledgment section was modified in the version published ASAP October 4, 2008; the corrected version published ASAP October 30, 2008.

Supporting Information Available

This information is available free of charge via the Internet at http://pubs.acs.org

Literature Cited

(1) Jansen, E.; Overpeck, J.; Briffa, K. R.; Duplessy, J.-C.; Joos, F.; Masson-Delmotte, V.; Olago, D. ; Otto-Bliesner, O.; Peltier, W. R.; Rahmstorf, S.; Ramesh, R.; Raynaud, D.; Rind, D.; Solomina, O.; Villalba, R.; Zhang, D. Palaeoclimate. In *IPCC 2007: Climate Change 2007 - The Physical Science Basis*; Solomon, S.; Qin, D.; Manning, M.; Chen, Z.; Marquis, M.; Averyt, K. B.; Tignor, M.; and Miller, H. L. Eds.; Cambridge University Press: Cambridge, 2007.

(2) EPICA community members. One-to-one coupling of glacial climate variability in Greenland and Antarctica *Nature* **2006**, *444*, 195−198.

(3) EPICA community members. Eight glacial cycles from an Antarctic ice core *Nature* **2004**, *429*, 623−628.

(4) Jacobson, M. C.; Hansson, H. C.; Noone, K. J.; Charlson, R. J. Organic atmospheric aerosols: Review and state of the science. *Rev. Geophys.* **2000**, *38*, 267–294.

(5) Novakov, T.; Penner, J. E. Large contribution of organic aerosols to cloud-condensation-nuclei concentrations. *Nature* **1993**, *365*, 823–826.

(6) Penner, J. E.; Dickinson, R. E.; Oneill, C. A. Effects of aerosol from biomass burning on the global radiation budget. *Science* **1992**, *256*, 1432–1434.

(7) Legrand, M.; Mayewski, P. Glaciochemistry of polar ice cores: A review. *Rev. Geophys.* **1997**, *35*, 219–243.

(8) Gelencsér, A. *Carbonaceous Aerosol*; Springer: Dordrecht, The Netherlands, 2004.

(9) Grannas, A. M.; Hockaday, W. C.; Hatcher, P. G.; Thompson, L. G.; Mosley-Thompson, E. New revelations on the nature of organic matter in ice cores. *J. Geophys. Res. (USA)* **2006**, *111*.

(10) Lyons, W. B.; Welch, K. A.; Doggett, J. K. Organic carbon in Antarctic snow. *Geophys. Res. Lett.* **2007**, *34*.

(11) Hutterli, M. A.; McConnell, J. R.; Bales, R. C.; Stewart, R. W. Sensitivity of hydrogen peroxide (H2O2) and formaldehyde (HCHO) preservation in snow to changing environmental conditions: Implications for ice core records. *J. Geophys. Res.* **2003**, *108*, 4023.

(12) Staffelbach, T.; Neftel, A.; Stauffer, B.; Jacob, D. A record of the atmospheric methane sink from formaldehyde in polar ice cores. *Nature* **1991**, *349*, 603–605.

(13) Bertler, N.; Mayewski, P. A.; Aristarain, A.; Barrett, P.; Becagli, S.; Bernardo, R.; Bo, S.; Xiao, C.; Curran, M.; Qin, D.; Dixon, D.; Ferron, F.; Fischer, H.; Frey, M.; Frezzotti, M.; Fundel, F.; Genthon, C.; Gragnani, R.; Hamilton, G.; Handley, M.; Hong, S.; Isaksson, E.; Kang, J.; Ren, J.; Kamiyama, K.; Kanamori, S.; Karkas, E.; Karlof, L.; Kaspari, S.; Kreutz, K.; Kurbatov, A.; Meyerson, E.; Ming, Y.; Zhang, M.; Motoyama, H.; Mulvaney, R.; Oerter, H.; Osterberg, E.; Proposito, M.; Pyne, A.; Ruth, U.; Simoes, J.; Smith, B.; Sneed, S.; Teinila, K.; Traufetter, F.; Udisti, R.; Virkkula, A.; Watanabe, O.; Williamson, B.; Winther, J. G.; Li, Y.; Wolff, E.; Li, Z.; Zielinski, A. Snow chemistry across Antarctica. *Ann. Glaciol.* **2005**, *41*, 167–179.

(14) Legrand, M.; Deangelis, M. Origins and variations of light carboxylic-acids in polar precipitation. *J. Geophys. Res.* **1995**, *100*, 1445–1462.

(15) Kawamura, K.; Suzuki, I.; Fujii, Y.; Watanabe, O. Historical records of fatty acids in an ice core from Site-J, Greenland. *Proc. NIPR Symp. Polar Meteorol. Glaciol.* **1995**, *9*, 1–11.

(16) Kawamura, K.; Suzuki, I.; Fujii, Y.; Watanabe, O. Ice core record of fatty acids over the past 450 years in Greenland. *Geophys. Res. Lett.* **1996**, *23*, 2665–2668.

(17) Kaufmann, P.; Federer, U.; Hutterli, M.; Bigler, M.; Schüpbach, S.; Ruth, U.; Stocker, T. F. A new Continuous Flow Analysis (CFA) system for high-resolution field measurements on ice cores. *Environ. Sci. Technol.* **2008**, *42*, 8044−8050.

(18) Röthlisberger, R.; Bigler, M.; Hutterli, M.; Sommer, S.; Stauffer, B.; Junghans, H. G.; Wagenbach, D. Technique for continuous high-resolution analysis of trace substances in firn and ice cores. *Environ. Sci. Technol.* **2000**, *34*, 338–342.

(19) Huber, C.; Leuenberger, M.; Zumbrunnen, O. Continuous extraction of trapped air from bubble ice or water for on-line determination of isotope ratios. *Analytical Chemistry* **2003**, *75*, 2324–2332.

(20) Sakamoto, T.; Miyasaka, T. Study confirming the accuracy of a method for measuring TOC by wet oxidation. *Ultrapure Water* **1987**, *4*, 24–31.

(21) Sugimura, Y.; Suzuki, Y. A high-temperature catalytic-oxidation method for the determination of non-volatile dissolved organic-carbon in seawater by direct injection of a liquid sample. *Mar. Chem.* **1988**, *24*, 105–131.

(22) Huber, S. A.; Frimmel, F. H. Flow-injection analysis of organic and inorganic carbon in the low-ppb range. *Anal. Chem.* **1991**, *63*, 2122–2130.

(23) Her, N.; Amy, G.; Foss, D.; Cho, J.; Yoon, Y.; Kosenka, P. Optimization of method for detecting and characterizing NOM by HPLC-size exclusion chromatography with UV and on-line DOC detection. *Environ. Sci. Technol.* **2002**, *36*, 1069–1076.

(24) Golimowski, J.; Golimowska, K. UV-photooxidation as pre-treatment step in inorganic analysis of environmental samples. *Anal. Chim. Acta* **1996**, *325*, 111–133.

(25) Perry, R. H. G, D. W. *Perry's Chemical Engineers' Handbook*, 7ed.; McGraw-Hill: New York, 1997.

(26) Siemer, D. D.; Johnson, V. J. Silicone-rubber tubing for elimination of background conductivity in anion chromatography. *Anal. Chem.* **1984**, *56*, 1033–1034.

(27) Stumm, W. a, J. M. *Aquatic Chemistry*; Wiley: New York, 1981.

(28) Grannas, A. M.; Shepson, P. B.; Filley, T. R. Photochemistry and nature of organic matter in Arctic and Antarctic snow. *Global Biogeochem. Cycles* **2004**, *18*.

(29) Frezzotti, M.; Bitelli, G.; De Michelis, P.; Deponti, A.; Forieri, A.; Gandolfi, S.; Maggi, V.; Mancini, F.; Remy, F.; Tabacco, I. E.; Urbini, S.; Vittuari, L.; Zirizzottl, A. Geophysical survey at Talos Dome, East Antarctica: the search for a new deep-drilling site. *Ann. Glaciol.* **2004**, *39*, 423–432.

(30) Legrand, M.; Ducroz, F.; Wagenbach, D.; Mulvaney, R.; Hall, J. Ammonium in coastal Antarctic aerosol and snow: Role of polar ocean and penguin emissions. *J. Geophys. Res., [Atmos.]* **1998**, *103*, 11043–11056.

(31) Wolff, E. W.; Fischer, H.; Fundel, F.; Ruth, U.; Twarloh, B.; Littot, G. C.; Mulvaney, R.; Rothlisberger, R.; de Angelis, M.; Boutron, C. F.; Hansson, M.; Jonsell, U.; Hutterli, M. A.; Lambert, F.; Kaufmann, P.; Stauffer, B.; Stocker, T. F.; Steffensen, J. P.; Bigler, M.; Siggaard-Andersen, M. L.; Udisti, R.; Becagli, S.; Castellano, E.; Severi, M.; Wagenbach, D.; Barbante, C.; Gabrielli, P.; Gaspari, V. Southern Ocean sea-ice extent, productivity and iron flux over the past eight glacial cycles. *Nature* **2006**, *440*, 491–496.

(32) Bigler, M.; Rothlisberger, R.; Lambert, F.; Stocker, T. F.; Wagenbach, D. Aerosol deposited in East Antarctica over the last glacial cycle: Detailed apportionment of continental and sea-salt contributions. *J.f Geophys. Res., [Atmos.]* **2006**, *111*.

(33) Twickler, M. S.; Spencer, M. J.; Lyons, W. B.; Mayewski, P. A. Measurement of organic-carbon in polar snow samples. *Nature* **1986**, *320*, 156–158.

(34) Skidmore, M.; Anderson, S. P.; Sharp, M.; Foght, J.; Lanoil, B. D. Comparison of microbial community compositions of two subglacial environments reveals a possible role for microbes in chemical weathering processes. *Appl. Environ. Microbiol.* **2005**, *71*, 6986–6997.

ES801244E